PAPER

Ultrathin-film optical coating for angle-independent remote hydrogen sensing

IOP Publishing Measurement Science and Technology
Meas. Sci. Technol. **31** (2020) 115201 (6pp) https://doi.org/10.1088/1361-6501/ab9fd8

Ultrathin-film optical coating for angle-independent remote hydrogen sensing

Mohamed ElKabbash[1,2], Kandammathe Valiyaveedu Sreekanth[1], Arwa Fraiwan[3], Jonathan Cole[4], Yunus Alapan[3], Theodore Letsou[1], Nathaniel Hoffman[1], Chunlei Guo[2], R Mohan Sankaran[4], Umut A Gurkan[3,5,6,7], Michael Hinczewski[1] and Giuseppe Strangi[1,8,9]

[1] Department of Physics, Case Western Reserve University, 10600 Euclid Avenue, Cleveland, OH 44106, United States of America
[2] The Institute of Optics, University of Rochester, Rochester, NY 14627, United States of America
[3] Case Biomanufacturing and Microfabrication Laboratory, Mechanical and Aerospace Engineering Department, Case Western Reserve University, Cleveland, OH 44106, United States of America
[4] Department of Chemical and Biomolecular Engineering, Case Western Reserve University, Cleveland, OH United States of America
[5] Biomedical Engineering Department, Case Western Reserve University, Cleveland, OH 44106, United States of America
[6] Department of Orthopedics, Case Western Reserve University, Cleveland, OH 44106, United States of America
[7] Advanced Platform Technology Center, Louis Stokes Cleveland Veterans Affairs Medical Center, Cleveland, OH 44106, United States of America
[8] CNR-NANOTEC, Istituto di Nanotecnologia and Department of Physics, University of Calabria, Rende, Italy
[9] Istituto Italiano di Tecnologia, Via Morego 30, 16163, Genova, Italy

E-mail: mke23@case.edu and gxs284@case.edu

Received 14 January 2020, revised 22 May 2020
Accepted for publication 24 June 2020
Published 25 August 2020

Abstract

We demonstrated an optically-active antireflection, light absorbing, optical coating as a hydrogen gas sensor. The optical coating consists of an ultrathin 20 nm thick palladium film on a 60 nm thick germanium layer. The ultrathin thickness of the Pd film (20 nm) mitigates mechanical deformation and leads to robust operation. The measurable quantities of the sensors are the shift in the reflection minimum and the change in the full width at half maximum of the reflection spectrum as a function of hydrogen gas concentration. At a hydrogen gas concentration of 4%, the reflection minimum shifted by ~46 nm and the FWHM increased by ~228 nm. The sensor showed excellent sensitivity, demonstrating a 6.5 nm wavelength shift for 0.7% hydrogen concentration, which is a significant improvement over other nanophotonic hydrogen sensing methods. Although the sensor's response showed hysteresis after cycling hydrogen exposure, the sensor is robust and showed no deterioration in its optical response after hydrogen deintercalation.

Keywords: anti-reflection coatings, hydrogen sensing, light absorbers, thin-films

(Some figures may appear in colour only in the online journal)

1. Introduction

Optical coatings are present in almost every optical instrument, with widespread applications ranging in displays and lighting [1, 2], to anticounterfeiting [3], and photovoltaics [4]. Recently, absorptive, anti-reflective optical coatings were developed where either transmission is not of importance, e.g. for structural coloring [5], and for the realization of generalized Brewster angle effect [6], or where high absorption is desired, e.g. for heat-assisted magnetic recording [7], solar-thermal power generation [8], and radiative cooling [9].

Light absorption is realized in optical coatings when light is critically coupled to the resonator, i.e. the absorption rate is equal to the reflection and transmission rates. This occurs when the interfering waves are out of phase (phase condition), and the out-of-phase waves are of equal amplitude (amplitude condition) [10, 11]. For ultrathin film optical coatings light absorbers, critical light coupling is typically achieved by two strategies; (1) using a lossy dielectric on a highly reflective substrate [12], e.g. Ag, Au, or Al, or (2) using a lossless dielectric on a low-reflectance substrate [13], e.g. Ni, Ti, or Pd. In addition, it has been shown that dielectrics with high refractive index lead to angle-independent light absorption [11]. Angle-independent light absorption leads to robust operation of optical coatings even on rough surfaces such as unpolished glass or paper [14].

On the other hand, hydrogen sensing is of crucial importance to industries where hydrogen gas (H_2) is present, e.g. in nuclear power stations, coal mines, lighting industry, and semiconductor manufacturing, etc [11]. Hydrogen is flammable with low ignition energy at concentrations from 4% to 75% [15]. Hydrogen sensors must be able to provide strong response to concentrations significantly lower than the explosive level of 4% to provide adequate warning before an explosion hazard takes place [16]. Although there exist many well-established hydrogen sensing technologies by measuring, e.g. the change in resistance of Pd wires [17], photonic-based hydrogen sensing is especially attractive as it allows for remote optical interrogation where the raw signal is optical instead of electrical. Photonic hydrogen sensors avoid the risk of being a possible source of ignition if a hydrogen leaks occurs [18].

Several systems have been reported as a platform for optical hydrogen sensing [15, 19]. In general, photonic-based hydrogen sensors measure changes in the refractive index of materials that form hydrides, i.e. they are hydride-based refractometers [20], most commonly using Pd. When Pd is exposed to H_2, it forms palladium hydride, PdH_x, which has a different complex refractive index than Pd that depends on the hydrogen stoichiometry [21]. At low H_2 concentrations, the intercalated hydrogen atoms are randomly situated inside the Pd lattice, forming a solid solution (α phase) [22]. At higher H_2 concentrations, the hydrogen atoms are ordered in the lattice forming a hydride β phase [23], which leads to an increase in the lattice parameter by ~3.5% and an expansion of the Pd film. The resulting tensile stress causes mechanical deformation and the formation of cracks can significantly degrade sensor performance over time [16].

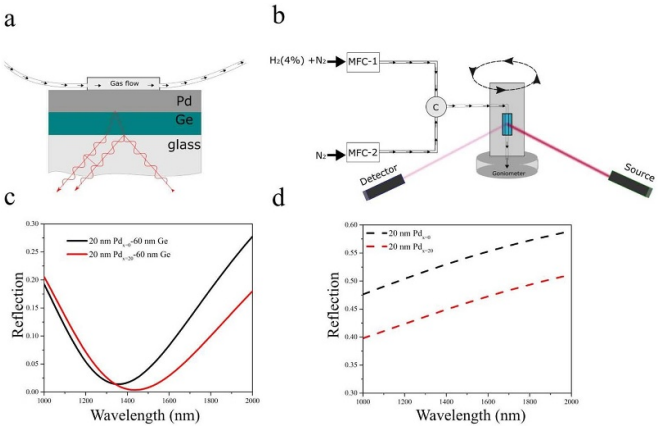

Figure 1. (a) A schematic of the optical coating sensor. The microfluidic channel is attached to the top of the Pd film to expose Pd to hydrogen. (b) The microfluidic channel is connected to two mass flow controllers (MFCs). One MFC controls the flow of nitrogen mixed with hydrogen (4% in concentration) and another MFC controls the flow of pure nitrogen. The sensor is placed on a variable-angle ellipsometer to measure the angular reflectivity. Calculated reflectance of (c) Pd-Ge optical coating and (d) a Pd film, for hydrogen atomic ratio x = 0 (black line), x = 20% (red line).

The formation of hydrides leads to a decrease in the absolute value of both the real and imaginary components of the complex refractive index of Pd [15]. Changes in Pd dielectric constant can be measured by directly measuring small changes in reflection [6], or scattering of Pd nanoparticles [24]. In addition, formation of hydrides can be measured indirectly by coating Pd on an optical fiber and measuring the changes in the output signal [25] or measuring the scattering of a plasmonic nanoparticle that acts as a refractometer [26]. In the context of thin Pd films, optical hydrogen sensing was demonstrated based on directly measuring changes in reflection [20] or transmission [27] due to hydride formation.

In this work, we demonstrate a nanophotonic hydrogen sensor based on an antireflective (absorptive) optical coating that suppresses light reflection in the telecommunication wavelength range. The dielectric-metal antireflective absorptive coating consists of a Ge and Pd ultrathin film. The ultrathin thickness of Pd mitigates mechanical deformation in Pd-based hydrogen sensors by reducing the clamping effect [28]. The Pd film forms a Pd hydride upon exposure to hydrogen which alters the wavelength of minimum reflection, λ_{min}, and the full width at half maximum (FWHM) of the light absorber. The measured shift in λ_{min} is ~46 nm at the critical H_2 concentration of 4%, which is significantly higher than other nanophotonic gas sensors [15, 19]. Due to the high refractive index of Ge, λ_{min} is angle independent over a wide range of angles ($25° - 45°$), and the shift in λ_{min} is approximately the same for all the measured incident angles. We show that the change in FWHM is an important sensing parameter reaching up to 228 ± 4 nm at 45°. The demonstrated sensor is inexpensive and can be deposited over a large area which enables scalable hydrogen monitoring [20].

2. Experimental

2.1. Sensor fabrication

The sensor consisted of a 20 nm thick Pd film on top of a 60 nm thick Ge layer, each deposited by electron beam evaporation at a rate of 0.5 Å s^{-1}on a 1 mm thick glass slide (see figure 1(a)). The Pd thickness was chosen to be ~20 nm to mitigate mechanical deformation by the clamping effect where the tensile stiffness of a film is inversely proportional to its thickness [15]. We chose Ge to serve as a dielectric as it has a high refractive index in the near infrared NIR region with negligible optical losses [29]. As we showed previously, a high index dielectric results in angle-independent light absorption in thin-film absorbers [14]. The Ge thickness was chosen to obtain a reflection minimum within the telecom wavelength windows (~1300 nm-1600 nm). To expose the sensor to hydrogen, we fabricated a microfluidic channel on the sensor (see figure 1(a)). The channel consists of a poly (methyl methacrylate) (PMMA) body (encompassing laser micromachined inlets and outlets) and a double-sided 100-μm adhesive film defining the outlines and thickness of the microchannel. The microfluidic channel was attached to the Pd side and the reflection was interrogated from the glass side.

2.2. Experimental setup

The sensor was placed on a variable angle ellipsometer (J A Woollam) to measure the angular reflectance R (figure 1(b)). To control the hydrogen concentration, a 4% hydrogen (H_2) in nitrogen (N_2) mixture was diluted by pure N_2. The ratio of the two was varied by two digital mass flow controllers (MFCs) to obtain a final concentration between 0.7 and 4%. The reflection before introducing the hydrogen was measured and recorded. It is important to note that using an ellipsometer is ideal to perform angular reflectance measurement over a wide wavelength range, however, it limits our ability to determine the exact response time of the sensor. In all cases, the response time of a hydrogen sensor depends on the hydrogen diffusion coefficient in the active material, here Pd, and the film thickness [30]. For the purpose of our experiments, we recorded the reflection ~12 min after introducing the H_2/N_2 mixture to ensure that we observe the steady state reflection.

3. Theoretical background

To understand the sensing mechanism, we investigated how the optical properties of our absorber depend on wavelength. The system of interest can be defined as a glass substrate with a refractive index n_0 (glass), a lossless dielectric layer with thickness h and refractive index n_D (Ge), and a lossy substrate with refractive index $n_S + ik_S$ (Pd). Light is incident on the system with wavelength, λ, and incident angle, θ. Following the theory described in [14], we can express the conditions for perfect absorption as

$$\tan \emptyset_D = \frac{(n_S - \gamma_0)\gamma_D}{k_S \gamma_0} = \frac{k_S \gamma_D}{\gamma_D^2 - n_S \gamma_0}, \quad (1)$$

where $\gamma_0 = n_0/\cos\theta$, $\gamma_D = n_D^2/\sqrt{n_D^2 - n_0^2 sin^2\theta}$, and $\emptyset_D = 2\pi h n_D^2/(\lambda\gamma_D)$. The latter is the phase gain in one pass through the dielectric layer. Note that to derive the above expressions, we assumed $|n_0 \sin\theta/(n_S + ik_S)|^2 \ll 1$, which is valid for the system under consideration. Both equalities in the equation above must be simultaneously satisfied for perfect absorption to occur. In the simplest scenario, we can ignore the dependence of n_0 and n_D on λ, so that we can rewrite the conditions for perfect light absorption directly in terms of λ_{min}:

$$\lambda_{min} = \frac{2\pi h n_D^2}{\gamma_D \left[m\pi + \tan^{-1}\left(\frac{(n_S - \gamma_0)\gamma_D}{k_S \gamma_0}\right)\right]}, \quad (2)$$

where m is an integer. Equation (2) shows that as n_S and k_S vary, the value of λ_{min} where perfect absorption takes place will also shift. Even if this is not the case, equation (2), still serves as an approximation for how λ_{min} changes. Clearly, changes in n_S and k_S of the metallic substrate can lead to a strong shift in λ_{min}. In addition, for a thin-film light absorber, the absorption linewidth depends on the reflectance from each interface where broader absorption modes are obtained for metallic films with lower reflectance [31]. To confirm our expectations, we performed a transfer matrix method calculation to calculate the reflection of the proposed Pd-Ge optical coating for hydrogen atomic ratio x = 0 and 20% (figure 1(c)). The calculated shift in reflection minimum λ_{min} is 90 nm and the full width at half maximum increased by ~200 nm. Conversely, the traditional direct measurement of the change in reflection of a Pd film, monitored from the glass slide, would lead to ~8% change in reflection as shown in figure 1(d). The incident light is p-polarized for all the calculations and measurements presented in this manuscript. We note here that the thin film interference-based hydrogen sensing differs from hydrogen sensing by coating Pd or other chemochromic oxides coated onto the tip or along the length of an optical fiber that is later detected by means of interferometry [31]. In the latter case, Pd coats a small portion of the fiber and upon hydrogen exposure and lattice expansion, the fiber's effective optical path length changes [15].

4. Results and discussion

Figure 2(a) shows the measured reflection spectrum of the optical coating over the wavelength range 1000–2000 nm at 25^0 (top panel), 35^0 (middle panel), and 45^0 (bottom panel). We first note that λ_{min} occurs at similar wavelengths regardless of the incident angle. After introducing H_2 at 4% concentration, we see a clear shift in λ_{min}. The total shifts in λ_{min} are 46 ± 2 nm, 47 ± 2 nm, and 45 ± 2 nm, at $25^0, 35^0$, and 45^0, respectively. The angle-independent sensitivity is an interesting property of the demonstrated sensor.

Figures 2(b) and (c) show contour maps of the angular reflectance for our sensors exposed to N_2 only and to H_2 (4% in N_2), respectively. In addition to the wavelength

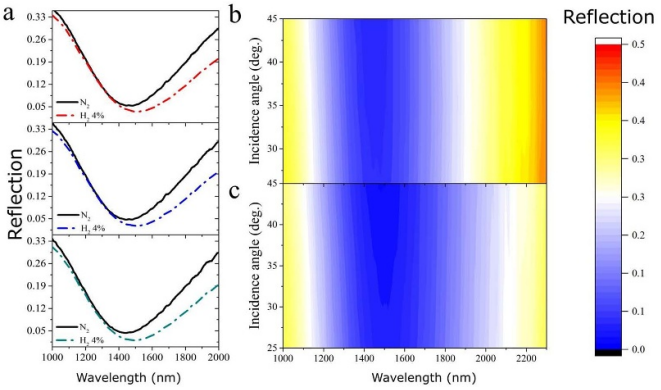

Figure 2. (a) Reflection measurements for the optical absorber before and after introducing hydrogen with C = 4% for three different incident angles 25°, 35°, and 45°. A contour plot of the angular reflection shows the angular reflection of the absorber for (b) C = 0% and (c) C = 4%. The FWHM increases significantly after introducing hydrogen for all incident angles.

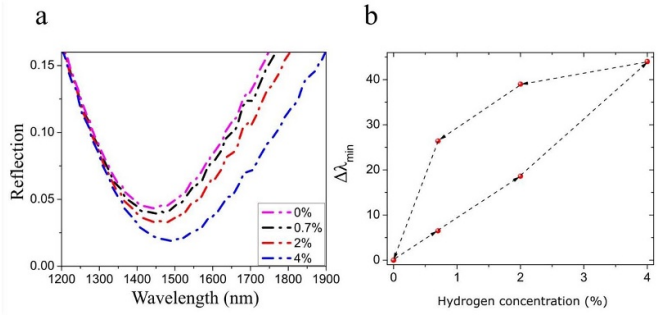

Figure 3. (a) Reflection of the absorber as a function of hydrogen concentration. (b) Sensor response to hydrogen concentrations (0.7%–4%) showing hysteresis behavior in reflectivity minimum, λ_{min}.

shifts, the FWHMs of the absorption modes significantly increase in the presence of H_2. The changes in the FWHM are 195 ± 4 nm, 186 ± 4 nm, and 228 ± 4 nm, at $25^0, 35^0$, and 45^0 respectively. The change in the FWHM can be measured by monitoring changes in the reflection intensity of a broadband NIR light source, e.g. using Tungsten halogen and Krypton lamps. Sensors that rely on changes in the intensity may offer a cheaper alternative as they do not require using a spectrometer. For a broadband detector, the reflected power can be calculated as

$$P = \int^{\frac{hc}{\lambda}} R(\lambda)\, d\lambda, \tag{3}$$

where h and c are the Planck's constant and speed of light and $R(\lambda)$ is the spectral reflection of the sample. We can then calculate the percent power difference before and after introducing the hydrogen as follows:

$$\Delta P = \frac{P_{N2} - P_{H2}}{P_{H2}} \times 100, \tag{4}$$

where P_{N2} and P_{H2} are the reflected power from the sensor before and after introducing hydrogen, respectively. The increase in the FWHM due to introducing hydrogen is tantamount to a decrease in the total reflected power. The calculated ΔP is ~25%, 28%, and 33% for a hydrogen concentration of 4% and an incident angle of 25°, 35°, and 45°, respectively.

We note that the change in the FWHM of the optical coating hydrogen sensor is an additional advantage over Fabry–Perot cavity hydrogen sensor which shows small overall change in the FWHM [15]. Furthermore, Fabry–Perot hydrogen sensors rely on cavity resonances which requires a dielectric with an optical thickness of at least λ/2 which requires excessively thick dielectric films when operating at longer wavelengths.

Figure 3(a) shows the shift in reflection at an incidence angle of 45° as a function of hydrogen concentration. We obtained shifts of 6.5 nm, 18.6 nm, and 44 nm at concentrations of 0.7%, 2%, and 4%, respectively. We note that the lowest hydrogen concentration used was determined based on the MFC control range and do not represent the lowest concentration that can be detected. For comparison, previous works showed ultrasensitive optical hydrogen sensing with ~2.5 nm shift in wavelength for 0.6% hydrogen concentration [32]. In our work, we demonstrate 6.5 nm shift for 0.7%.

We also studied the hysteresis behavior of the sensor. In general, when Pd forms a hydride, a mechanical energy barrier is created due to the coherency strain produced by the lattice expansion of the hydride phase [6]. This barrier prevents the release of hydrogen atoms situated inside the hydride lattice to recover the original Pd structure. Figure 3(b) shows a hysteresis plot for the shift in λ_{min} at different H_2 concentrations (0%, 0.7%, 2% and 4%) and 45° incidence angles. Each measurement presented is extracted from the steady state reflection spectrum which was obtained after ~12 min for each concentration. The λ_{min} is found to be higher when the H_2 concentration is decreased than when the H_2 concentration is increased. We suggest that the hydrogen content or stoichiometries in terms of x in the PdH_x are different during the forward and reverse cycles of exposing to different H_2 concentrations, with the stoichiometry being higher in the reverse cycle because of the aforementioned mechanical energy barrier to deintercalation from coherency strain. We note here that heating the sensor to higher temperatures could limit or eliminate the observed hysteresis, however, on the expense of minimizing the sensitivity [33, 34]. Moreover, using Pd alloys was shown to minimize the hysteresis significantly, e.g. using Pd Au alloys [35, 36]. The existence of coherency strain, however, did not affect the overall performance of our sensor as the absorption mode relaxed to the initial λ_{min} when the H_2 concentration was decreased to zero (pure N_2).

5. Conclusion

In summary, we developed an ultrathin film optical coating for hydrogen sensing. The sensor consists of an antireflective, absorptive Pd film. The change in the antireflection properties in terms of reflection minimum and FWHM enabled the

detection of low hydrogen concentrations. The sensor shows similar overall shift in reflection minimum over a broad range of incidence angles. Hysteresis in the reflection minimum was found arising from a mechanical energy barrier to deintercalation but did not lead to degradation in the sensor performance. The hysteresis issue can be potentially mitigated by employing different types of Pd alloys as substrates. Moreover, using Pd alloys with higher hydrogen diffusion coefficients or using a substrate consisting of Pd nanowire mesh [37] can provide a sensor with a short response time.

Acknowledgments

G S received funding from the Ohio Third Frontier Project 'Research Cluster on Surfaces in Advanced Materials (RCSAM) at Case Western Reserve University' and the GU Malignancies Program of the Case Comprehensive Cancer Centre and was supported in part by the National Science Foundation, Grant Nos. DMR-1708742. G. S., M. H., and U. A. G. acknowledge the support of the National Science Foundation, Award #1904592. U.A.G. acknowledges, and National Science Foundation CAREER Award #1552782. This article's contents are solely the responsibility of the authors and do not necessarily represent the official views of the National Institutes of Health.

Conflict of interest

The authors declare no conflicts of interest.

ORCID iDs

Mohamed ElKabbash https://orcid.org/0000-0003-3795-7714
Arwa Fraiwan https://orcid.org/0000-0002-7745-409X
Yunus Alapan https://orcid.org/0000-0003-3064-7342
Nathaniel Hoffman https://orcid.org/0000-0002-8865-2286
R Mohan Sankaran https://orcid.org/0000-0002-9399-4790
Umut A Gurkan https://orcid.org/0000-0002-0331-9960
Michael Hinczewski https://orcid.org/0000-0003-2837-7697
Giuseppe Strangi https://orcid.org/0000-0002-7509-2048

References

[1] Macleod H A 1986 *Thin Film Optical Filters* 4th edn (London Adam Hilger)
[2] Tannas L E 1989 Flat-panel displays displace large, heavy, power-hungry CRTs *IEEE Spectr.* **26** 34–35
[3] Hornbeck L J 1997 *Digital Light Processing for High-Brightness High-Resolution Applications* vol 3013 EI (SPIE)
[4] Dobrowolski J A, Ho F C and Waldorf A 1989 Research on thin film anticounterfeiting coatings at the national research council of Canada *Appl. Opt.* **28** 2702–17
[5] Chen D 2001 Anti-reflection (AR) coatings made by sol–gel processes: a review *Sol. Energy Mater. Sol. Cells* **68** 313–36
[6] Letsou T, ElKabbash M, Iram S, Hinczewski M and Strangi G 2019 Heat-induced perfect light absorption in thin-film metasurfaces for structural coloring [Invited] *Opt. Mater. Express* **9** 1386–93
[7] Sreekanth K V *et al* 2019 Generalized brewster angle effect in thin-film optical absorbers and its application for graphene hydrogen sensing *ACS Photon.* **6/7** 1610–17
[8] Deng C *et al* 2018 Nanocavity induced light concentration for energy efficient heat assisted magnetic recording media *Nano Energy* **50** 750–5
[9] ElKabbash M *et al* 2017 Tunable black gold: controlling the near-field coupling of immobilized au nanoparticles embedded in mesoporous silica capsules *Adv. Opt. Mater.* **5** 1700617
[10] Raman A P, Anoma M A, Zhu L, Rephaeli E and Fan S 2014 Passive radiative cooling below ambient air temperature under direct sunlight *Nature* **515** 540
[11] ElKabbash M, Iram S, Letsou T, Hinczewski M and Strangi G 2018 Designer perfect light absorption using ultrathin lossless dielectrics on absorptive substrates *Adv. Opt. Mater.* **6** 1800672
[12] Kats M A and Capasso F 2016 Optical absorbers based on strong interference in ultra-thin films *Laser Photon. Rev.* **10** 735–49
[13] Kats M A, Blanchard R, Genevet P and Capasso F 2012 Nanometre optical coatings based on strong interference effects in highly absorbing media *Nat. Mater.* **12** 20
[14] ElKabbash M *et al* 2017 Iridescence-free and narrowband perfect light absorption in critically coupled metal high-index dielectric cavities *Opt. Lett.* **42** 3598–601
[15] Hübert T, Boon-Brett L, Black G and Banach U 2011 Hydrogen sensors – a review *Sens. Actuators.* B **157** 329–52
[16] Fong N R, Berini P and Tait R N 2016 Hydrogen sensing with Pd-coated long-range surface plasmon membrane waveguides *Nanoscale* **8** 4284–90
[17] Pitts R, Liu P, Lee S-H and Tracy E 2001 Interfacial stability of thin film hydrogen sensors *proceedings of the 2001 DOE hydrogen program review*
[18] Sun Y and Wang H H 2007 High-performance, flexible hydrogen sensors that use carbon nanotubes decorated with palladium nanoparticles *Adv. Mater.* **19** 2818–23
[19] Tittl A *et al* 2011 Palladium-based plasmonic perfect absorber in the visible wavelength range and its application to hydrogen sensing *Nano Lett.* **11** 4366–9
[20] Liu N, Tang M L, Hentschel M, Giessen H and Alivisatos A P 2011 Nanoantenna-enhanced gas sensing in a single tailored nanofocus *Nat. Mater.* **10** 631
[21] Sreekanth K V, ElKabbash M, Alapan Y, Ilker E I, Hinczewski M, Gurkan U A and Strangi G 2017 Hyperbolic metamaterials-based plasmonic biosensor for fluid biopsy with single molecule sensitivity *EPJ Appl. Metamater.* **4** 1
[22] Vargas W E, Rojas I, Azofeifa D E and Clark N 2006 Optical and electrical properties of hydrided palladium thin films studied by an inversion approach from transmittance measurements *Thin Solid Films* **496** 189–96
[23] Syrenova S *et al* 2015 Hydride formation thermodynamics and hysteresis in individual Pd nanocrystals with different size and shape *Nat. Mater.* **14** 1236
[24] Cheng Y-T, Li Y, Lisi D and Wang W M 1996 Preparation and characterization of Pd/Ni thin films for hydrogen sensing *Sens. Actuators.* B **30** 11–16
[25] Wadell C, Syrenova S and Langhammer C 2014 Plasmonic hydrogen sensing with nanostructured metal hydrides *ACS Nano* **8** 11925–40

[26] Zhang Y-N *et al* 2017 Recent advancements in optical fiber hydrogen sensors *Sens. Actuators.* B **244** 393–416
[27] Zhao Z, Carpenter M, Xia H and Welch D 2006 All-optical hydrogen sensor based on a high alloy content palladium thin film *Sens. Actuators.* B **113** 532–8
[28] Cheong H, Young Shim J, Dong Lee J, Mo Jin J and Lee S-H 2009 Comparison of Pd, Pt and Pt/Pd as catalysts for hydrogen sensor films *J. Korean Phys. Soc.* **55** 2693
[29] Lee E, Lee J M, Koo J H, Lee W and Lee T 2010 Hysteresis behavior of electrical resistance in Pd thin films during the process of absorption and desorption of hydrogen gas *Int. J. Hydrog. Energy* **35** 6984–91
[30] Liu Y, Li Y, Huang P, Song H and Zhang G 2016 Modeling of hydrogen atom diffusion and response behavior of hydrogen sensors in Pd–Y alloy nanofilm *Sci. Rep.* **6** 37043
[31] Li Z, Butun S and Aydin K 2015 Large-area, lithography-free super absorbers and color filters at visible frequencies using ultrathin metallic films *ACS Photon.* **2** 183–8
[32] Jiang R, Qin F, Ruan Q, Wang J and Jin C 2014 Ultrasensitive plasmonic response of bimetallic Au/Pd nanostructures to hydrogen *Adv. Funct. Mater.* **24** 7328–37
[33] Lewis F 1994 Palladium-hydrogen system *Platinum Met. Rev.* **38** 112–8
[34] Fisser M, Badcock R A, Teal P D and Hunze A 2018 Optimizing the sensitivity of palladium based hydrogen sensors *Sens. Actuators.* B **259** 10–19
[35] Bannenberg L J, Nugroho F A A, Schreuders H, Norder B, Trinh T T, Steinke N-J, van Well A A, Langhammer C and Dam B 2019 Direct comparison of PdAu alloy thin films and nanoparticles upon hydrogen exposure *ACS Appl. Mater. Interfaces* **11** 15489–97
[36] Luo S, Wang D and Flanagan T B 2010 Thermodynamics of hydrogen in fcc Pd− Au alloys *J. Phys. Chem.* B **114** 6117–25
[37] Zeng X Q *et al* 2011 Hydrogen gas sensing with networks of ultrasmall palladium nanowires formed on filtration membranes *Nano Lett.* **11** 262–8